

Applying a global pulse disturbance to eliminate spiral waves in models of cardiac muscle

Jian Gao(高见), Changgui Gu(顾长贵), and Huijie Yang(杨会杰)
Citation: Chin. Phys. B, 2021, 30 (**7**): 070501. DOI: 10.1088/1674-1056/abf553
Journal homepage: http://cpb.iphy.ac.cn; http://iopscience.iop.org/cpb

What follows is a list of articles you may be interested in

Effects of abnormal excitation on the dynamics of spiral waves

Min-Yi Deng(邓敏艺), Xue-Liang Zhang(张学良), Jing-Yu Dai(戴静娱)
Chin. Phys. B, 2016, 25 (**1**): 010504. DOI: 10.1088/1674-1056/25/1/010504

A cellular automaton model for the ventricular myocardium considering the layer structure

Deng Min-Yi, Dai Jing-Yu, Zhang Xue-Liang
Chin. Phys. B, 2015, 24 (**9**): 090503. DOI: 10.1088/1674-1056/24/9/090503

The effect of cellular aging on the dynamics of spiral waves

Deng Min-Yi, Chen Xi-Qiong, Tang Guo-Ning
Chin. Phys. B, 2014, 23 (**12**): 120503. DOI: 10.1088/1674-1056/23/12/120503

Motion of spiral tip driven by local forcing in excitable media

Liu Gui-Quan, Ying He-Ping
Chin. Phys. B, 2014, 23 (**5**): 050502. DOI: 10.1088/1674-1056/23/5/050502

Feedback control of wave segments in excitable medium

Wu Ning-Jie, Gao Hong-Jun, Ying He-Ping
Chin. Phys. B, 2013, 22 (**5**): 050501. DOI: 10.1088/1674-1056/22/5/050501

Applying a global pulse disturbance to eliminate spiral waves in models of cardiac muscle*

Jian Gao(高见), Changgui Gu(顾长贵)†, and Huijie Yang(杨会杰)

Business School, University of Shanghai for Science and Technology, Shanghai 200093, *China*

(Received 2 February 2021; revised manuscript received 25 March 2021; accepted manuscript online 7 April 2021)

Removal of spiral waves in cardiac muscle is necessary because of their threat to life. Common methods for this removal are to apply a local disturbance to the media, such as a periodic forcing. However, most of these methods accelerate the beating of the cardiac muscle, resulting in the aggravation of the ventricular tachycardia, which directly threatens life. In the present study, in order to clear off spiral waves, a global pulse-disturbance is applied to the media based on three models of cardiac muscle. It is found that the spiral waves are eliminated and the frequency of the cardiac muscle is decreased in a short time, and finally, the state of the medium reaches the normal oscillation, which supports a target waves. Our method sheds light on the removal of spiral waves in cardiac muscle and can prevent the ventricular tachycardia as well as the ventricular fibrillation.

Keywords: ventricular fibrillation, spiral wave, pattern formation, elimination

PACS: 05.45.Xt, 47.54.–r, 82.40.Bj, 89.75.–k **DOI:** 10.1088/1674-1056/abf553

1. Introduction

Sudden cardiac death is a major cause accounting for over 300000 deaths per year in the USA alone.[1] Under normal conditions, cardiac action potentials originated from the sinoatrial node periodically propagate at a rate of about 75 bpm in tissues.[2,3] In abnormal situations, such as during the initiation of ventricular tachycardia (VT), reentry of the propagation occurs in that a spiral wave emerges. The wave may stay as a stable spiral wave or degenerate into small fragments of waves, i.e., ventricular fibrillation (VF) resulting from a turbulent cardiac electrical activity, which is a major reason for sudden cardiac death.[4,5] During the VF event, the heart is incapable of any concerted pumping action. These VT and VF events do not often terminate spontaneously.[6–8] The termination depends on the dynamic properties of the spiral wave.[9,10] Therefore, spiral waves in cardiac muscle play an essential role in VT and VF events. Consequently, removal of spiral waves is of much practical interest.[11–17]

At present, a common method of clinical treatment for cardiac tremor is electroshock, which can stimulate the thoracic cavity with high voltage electricity (about 4–7 kV). However, the electroshock method has many disadvantages, such as damage to heart tissue, pain to the patient, and low cure rate.[18] In the research of treatment of VT and VF, one of the research directions is spiral wave dynamics, attempting to find effective methods to remove and to suppress the spiral wave by studying the dynamic properties of the spiral wave. For instance, Gao *et al.*[19] proposed that the external forcing can suppress spiral waves and turbulence in excitable media, because the external forcing changes the excitability of the media. In Refs. [20,21], the authors reported that phase compression can suppress the spiral wave in excitable and oscillatory media. In Refs. [22,23] the authors studied the effects of electromagnetic induction on spiral waves and target waves in the model of cardiac tissue. Zhang *et al.*[24] proposed a method to eliminate spiral waves and spatiotemporal chaos using the synchronization transmission technology of network signals. Moreover, suppressing and controlling the pinned spiral wave are more difficult than the meandering spiral wave, because pinned spiral waves are often attracted to a local area (obstacle) such as heterogeneity. In the issue, in Refs. [25–28] researchers reported many effective schemes to control the pinned spiral waves. For instance, Chen *et al.*[28] have studied the behavior of spiral waves interacting with obstacles and the removal of pinned spiral waves by periodic mechanical deformation. In addition, some methods suppress spiral waves through competition of waves.[29–34] According to the wave competition rule,[35,36] it is required to impose a higher frequency wave to eliminate the spiral waves in excitable media. The appearance of such high-frequency waves will accelerate the beating of the cardiac muscle,[37] therefore, results in the aggravation of VT event. Accordingly, it is urgent to find a better alternative method for removal of spiral waves.

In this article, we propose a method to clear off spiral waves by exerting a global pulsating disturbance on the medium based on two models of cardiac muscle, i.e., the Fitzhugh–Nagumo (FHN) model[38] and the Bär model.[39] We also examine our method in the complex Ginzburg–Landau equation (CGLE) model.[40,41] The rest of the article

*Project supported by the National Natural Science Foundation of China (Grant Nos. 11875042 and 11505114), and the Shanghai project for construction of top disciplines (Grant No. USST-SYS01).

†Corresponding author. E-mail: gu_changgui@163.com

© 2021 Chinese Physical Society and IOP Publishing Ltd

is organized as follows. In Section 2, we introduce the models and the method. In Section 3 the numerical results are presented. The analytical results are given in Section 4. Lastly, conclusion and discussion are presented in Section 5.

2. Models and method

The two-dimensional (2D) cardiac tissue with trans-membrane current is often described by the FHN model expressed as follows:[38,42]

$$\begin{aligned} \frac{\partial A}{\partial t} &= \frac{f(A,B)}{\varepsilon} + I + D_A \nabla^2 A, \\ \frac{\partial B}{\partial t} &= \varepsilon g(A,B), \\ A(t_0^+) &= A(t_0^-) + \delta A, \quad t_0 = 0, \end{aligned} \tag{1}$$

where variable A is the trans-membrane potential, variable B is the slow variable for current, whose time ratio is ε, I is the external periodic forcing current, δA represents an increment of A of all local points obtained by an external one-off global pulse current, t_0 represents the moment when the pulse is applied, t_0^+ represents the moment when the pulse ends, t_0^- indicates the infinitesimal time before the pulse is applied, ∇^2 is $\partial^2/\partial x^2 + \partial^2/\partial y^2$, and the diffusion coefficient D_A is set to 1 for simplicity. The kinetics of this model are given by $f(A,B) = A - A^3/3 - B$ and $g(A,B) = A + \beta - \gamma B$. Here β and γ are parameters of the medium.

In the simulation, the chosen parameters for this excitable medium are $\varepsilon = 0.2$, $\beta = 0.5$, and $\gamma = 0.8$. Equation (1) with those parameters was also discussed in Ref. [21], showing that the medium can support a rigidly rotating spiral wave and the radius of the trajectory of spiral tip is zero. Our model is integrated on a 100×100 grid points with no-flux boundary conditions. A nine-point finite difference scheme is also applied to compute the Laplacian term $\nabla^2 A$, then the discrete equation is calculated via the four-order Runge–Kutta method. The space steps Δx and Δy are both 1, and the time step Δt is 0.01.

To simulate the electrical activity in a normal cardiac muscle, a pacemaker (external periodic forcing current) is placed in the center of the medium to form a stable target wave, and it reads

$$I = \begin{cases} I_0 \sin(2\pi\nu t), & r \le R, \\ 0, & r > R, \end{cases} \tag{2}$$

where I_0 and ν are the amplitude and frequency of the pacemaker, respectively, R represents the maximal radius of area driven by the pacemaker, and r represents the distance from the center of the pacemaker. The original site of the center of the pacemaker is set as $(x_0,\ y_0)$, and r is equal to $\sqrt{(x-x_0)^2 + (y-y_0)^2}$. The parameters of the pacemaker are set as $I_0 = 0.50$, $R = 2$, and $\nu = 0.60 \times 10^{-1}$. Note that the frequency of heartbeats here is normally less than the frequency during the initiation of VT caused by the spiral wave, which is 0.95×10^{-1}, so we let the frequency of the parameter be $\nu = 0.60 \times 10^{-1}$.

In order to facilitate the description of the effect of pulse, δA can be expressed as kA_0, i.e., $\delta A = kA_0$, where k represents a coefficient and A_0 (≈ 1.83) represents the amplitude of local oscillation. In this article, the moment of applying the pulse is assumed to be at the origin of time, i.e., $t_0 = 0$. In the following sections, we will examine the effects of the key parameter k, which indicates the degree of influence on the membrane potential of different ions.[38] Snapshots plotted in white and black describe the spatial distribution of the variable A. Because the gradient between the maximum value (white) and the minimum value (black) in the medium is so large, it is difficult to display the gray scale.

3. Numerical results

The general dynamics of the medium is shown in the supplementary files, including a target wave state and the appearance of spiral wave. We use the spiral waves in Fig. S1(b) in the supplementary files as the initial situation of the medium. To examine the effects of δA on the spiral, the value of k is gradually increased. Figure 1 shows the effects of the parameter k on the spiral. With the increase of k, although the stable spiral maintains in the medium, the position of the spiral tip differs (Figs. 1(a)–1(c)). In particular, the position of the center for $k = 0$ is indicated by a red solid point. When $k = 0.30$, the position of the center is slightly altered and close to the red solid point (Fig. 1(a)). When k is increased to 0.45 (Fig. 1(b)) or 0.60 (Fig. 1(c)), the position of the center is farther from the red point.

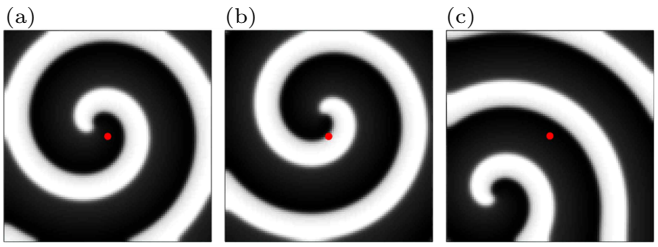


Fig. 1. The stabilized states of a spiral wave with selected values of k, (a) $k = 0.30$, (b) $k = 0.45$, (c) $k = 0.60$, respectively. The red point in the center of the medium indicates the location of the spiral center before the pulse is applied. Each snapshot is a part of the spirals in Fig. S1(b) in the supplementary files.

Interestingly, when k is further increased and exceeds the threshold $\bar{k}_1 = 0.63$, the spiral waves break into many smaller spiral waves (Fig. 2(a)). When k is further increased and exceeds (or is equal to) the threshold $\bar{k}_2 = 0.76$, the spiral wave is eliminated instantaneously, and a target wave is generated in the medium (Fig. 2(b)). Therefore, the parameter k affects the dynamic patterns of the medium.

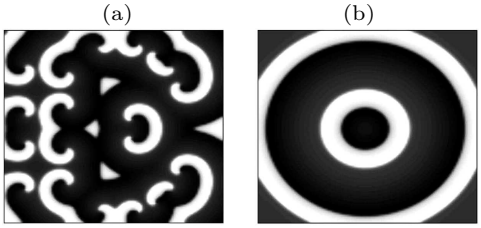


Fig. 2. The stabilized states of the medium with selected values of k, (a) $k = 0.70$, (b) $k = 0.77$, respectively.

In order to describe the effect of the parameter k on spiral waves in more detail, we show the relationship between the parameter k and the number of spiral tips in the medium (see Fig. 3). One can find that when k is in the interval $[0,\ 0.63]$, the number of spiral tip is 2, which means that the spiral waves are not broken or eliminated. When k is in the interval $(0.63,\ 0.76)$, the number of spiral tip is greater than 2, which means that the spiral waves are broken. When k is greater than or equal to 0.76, the number of spiral tip is 0, which means that the spiral waves are eliminated.

Further, we examine the temporal evolutions for the spiral after the disturbance is applied, if k is less than the threshold $\bar{k}_2 = 0.76$, and if k is greater than or equal to the threshold $\bar{k}_2$, respectively, in Fig. 4. Initially ($t = 0^-$), i.e., before the disturbance is applied, the stabilized spiral wave is observed. In Fig. 4(a), after the disturbance ($k = 0.70$) is applied, the spiral arms are divided into many small segments ($t = 5$), and then a number of smaller spiral waves are generated with each breakpoint as a new spiral tip ($t = 10$ and 25). In Fig. 4(b), after the disturbance ($k = 0.77$) is applied, the spirals ($t = 0^-$) suddenly disappear ($t = 5$ and 15), and a target wave is generated ($t = 25$). The temporal evolution in Figs. 4(a) and 4(b) are shown in Movie 1 and Movie 2 included in the supplementary files, respectively.

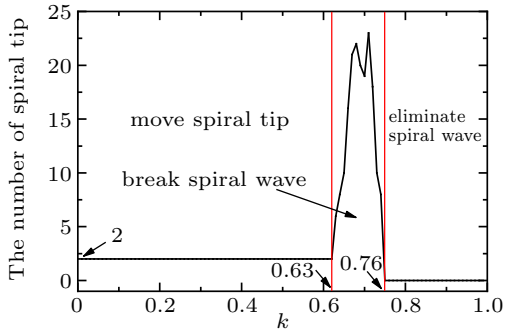


Fig. 3. The relationship between the parameter k and the number of spiral tip.

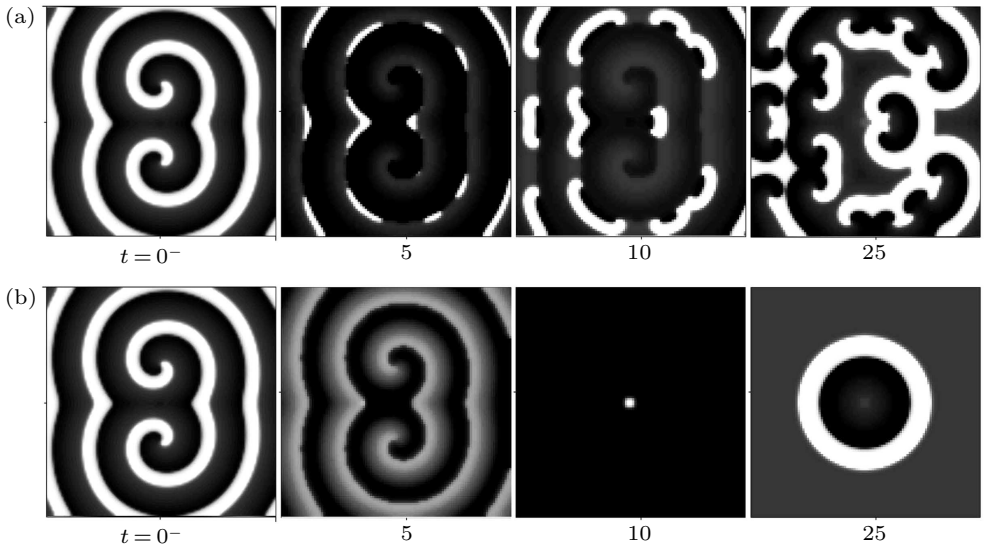


Fig. 4. The temporal evolution of spirals after the disturbance is applied, when $k = 0.70$ in (a) and $k = 0.77$ in (b), respectively. The moment when the disturbance is applied is the origin of time ($t = 0$).

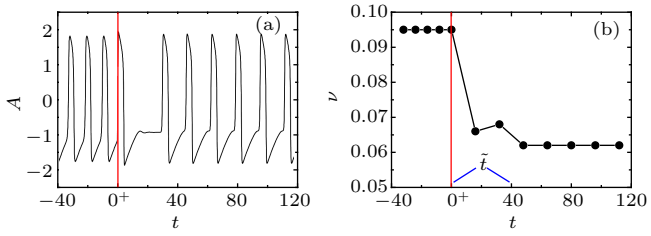


Fig. 5. Alternation of the state for a local oscillation before and after the disturbance ($k = 0.77$) is applied. (a) Temporal evolution of membrane potential A for a typical grid point (25, 25) in the medium. (b) Plots of ν versus t for the grid point (25, 25) in the medium, where ν is the frequency of this grid point.

The properties for a selected local oscillation, before and after δA is applied, are shown in Fig. 5, including the temporal evolution (a) and the corresponding frequency (b). Before the application ($t < 0$), the frequency is about 0.95×10^{-1}. After the disturbance is applied ($t \geq 0$), the frequency is quickly reduced to 0.60×10^{-1}. Interestingly, the duration for this reduction is about $\tilde{t} = 40$, which is about 2.5 times of the period of the target wave.

In addition to common spiral waves above, we also examine whether our method can suppress the pinned spiral waves, i.e., spiral waves, which are pinned (anchored) to localized

heterogeneities, are more difficult to suppress and control than the common spiral wave. In order to obtain the pinned spiral wave on the basis of Fig. 1(b), we operate on the medium: fix variables A in a small area near the spiral tip at -1.03 (potential of resting state). Figure 6(a) shows the pinned spiral waves. The temporal evolution of the pinned spiral waves is shown in Movie 3 in the supplementary files. After the pulse with $k = 0.77$ is applied, the pinned spiral waves are eliminated instantaneously, and a target wave is generated by the pacemaker in the medium of Fig. 6(b). The target wave can cross the obstacle and continue to spread. Movie 4 in the supplementary files shows the temporal evolution.

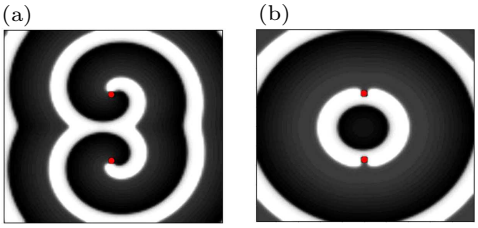


Fig. 6. (a) The pinned spiral waves, (b) a target wave with two localized heterogeneities. The red points are the localized heterogeneities.

In the supplementary files, we examine our method based on the Bär model and the CGLE model. We find that in these two models, through our method, the spiral tip can also be moved and the spiral wave can be eliminated.

4. Analytical results

There are several questions: Why can this method eliminate spiral waves? Why can the position of the spiral tip be moved when k is less than the threshold? In this section we try to explain.

To facilitate the analysis, we answer these questions based on the CGLE model (the model and numerical results are in the supplementary files). In Fig. 7(a), the point O, called the point defect, is the spiral center which is at the fixed point $(\mathrm{Re}(A), \mathrm{Im}(A)) = (0,0)$, the line Ω rotates counterclockwise with O as the center. Except the center point O, oscillations of all the other points are simple harmonic oscillation, and the closer to the center, the smaller the amplitude. The points (e.g., P_3 and P_3') that have the same distance from the O have the same phase trajectory. All local points (e.g., P_1, P_2 and P_3) in the radius r have the same phase, points in r' (e.g., P_3') and points in r (e.g., P_1, P_2 or P_3) exhibit an anti-phase synchronization, that is, the difference between their phases is π.

The spiral center is a self-sustaining wave source that does not require external action. To facilitate the analysis, we discretize the medium. Figure 8 shows nine oscillators near the spiral center in a discrete system, where $A_{(0,0)}$ is the point defect at the center of the spiral wave, and the oscillators symmetric about point O are anti-phase synchronous, i.e., $A_{(-1,1)} = -A_{(1,-1)}$, $A_{(-1,0)} = -A_{(1,0)}$, $A_{(-1,-1)} = -A_{(1,1)}$, $A_{(0,1)} = -A_{(0,-1)}$. $A_{(0,0)}$ is at the fixed point $(0,0)$. Since $A_{(0,0)} = 0$, their dynamic terms $A - (1+\mathrm{i}\beta)|A|^2 A = 0$. Now consider the diffusion term of $A_{(0,0)}$,

$$(1+\mathrm{i}\alpha)\nabla^2 A = (1+\mathrm{i}\alpha)\frac{A_{(0,1)} + A_{(0,-1)} + A_{(-1,1)} + A_{(1,0)} - 4A_{(0,0)}}{(\Delta x)^2} = 0.$$

Consequently, point O is always at the fixed point (0, 0), and the point defect can be self-sustaining, resulting in that the area near O is always in an uneven state, and this uneven state is what the self-sustaining wave source should satisfy. Moreover, disrupting the anti-phase synchronization around the point defect will break the existing balance, and completely breaking the anti-phase synchronization around the center of the spiral wave will cause the point defect to automatically collapse. Our method is to eliminate the spiral wave by breaking the anti-phase synchronization.

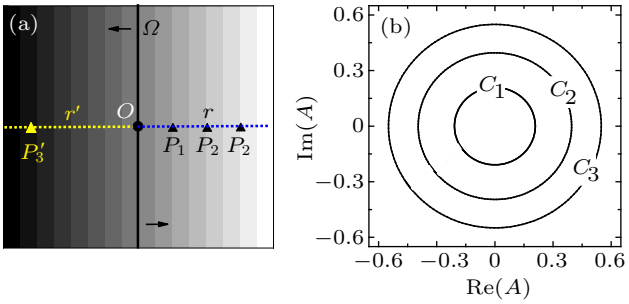


Fig. 7. The dynamic behavior near the spiral center: (a) A snapshot of a circular region near the center of the spiral. Point O is the center of the spiral, the black solid line Ω is a set of local points where $\mathrm{Re}(A)$ is 0, the black arrows indicate the direction of rotation of Ω. The blue dotted line r is any radius of this circular region, and the yellow dotted line r' is another radius on the same diameter. Points P_1, P_2 and P_3 are local points on r, P_3' is the symmetry point of P_3 relative to point O. P_1, P_2 and P_3 have the same phase, P_3 and P_3' are in anti-phase, i.e., the difference between their phase is π. (b) A phase diagram. Trajectories C_1 and C_2 in (b) are the phase trajectories of P_1 and P_2 in (a), respectively. C_3 is the phase trajectory of P_3 and P_3'.

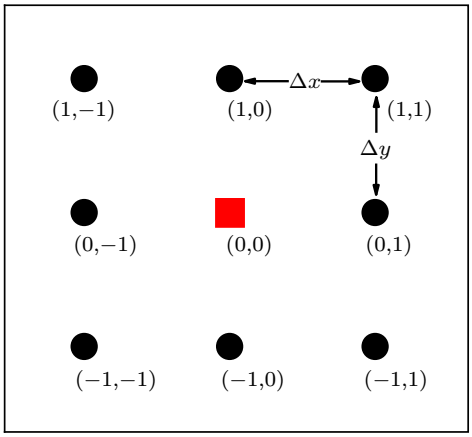


Fig. 8. Nine adjacent oscillators near the point defect in a discrete system. The circles and the square are adjacent local oscillators, the square is the point O in Fig. 5(a), Δx and Δy are the space steps.

Figure 9 shows the set of local points where the real or imaginary part of A is 0, which is called the symbol boundary

curve (SBC). The SBC is symmetric about point O before the δA is applied. The intersection (O) of the black solid line and the dotted line in Fig. 9 is the spiral center, i.e., the point defect, before δA is applied. After the disturbance is applied to the medium, the SBC of the real part loses its central symmetry and is close to one end of the SBC of the imaginary part, and the larger k, the closer to the SBC of the imaginary part (Fig. 9). For instance, the blue solid line in Fig. 9 is nearer to one end of the dotted line than the yellow and red ones. The alteration of the SBC of the real part, on the one hand, leads to the alteration of the position for the point defect, on the other hand, leads to the increase of the curvature of the SBC at the point defect (Fig. 9). For example, points O_1, O_2 and O_3 are the new point defects, the curvature at O_3 is greater than at O_2 and O_1. Simultaneously, the diffusion effect has a strong influence on the place where the curvature of the SBC is large, which causes the curvature to become smaller and smaller, resulting in further alteration of the position of the point defect.

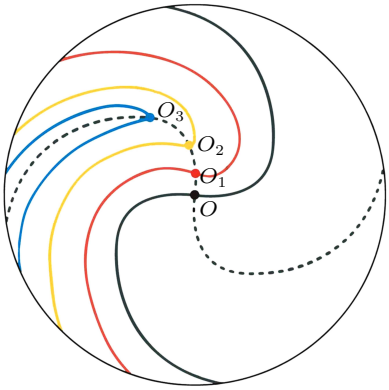


Fig. 9. The set of local points where $\mathrm{Re}(A) = 0$ and $\mathrm{Im}(A) = 0$. The black solid line and dotted line in are the SBCs of the real and imaginary parts of the initial spiral wave respectively. The red, yellow and blue solid lines, which are the SBCs of the real part after δA is applied, correspond to $k = 0.50$, $k = 0.85$ and $k = 0.92$, respectively. Point O is the point defect of the initial spiral wave, each of points O_1, O_2 and O_3 is point defect at $t = 0^+$ after δA is applied.

With our method, when $k < 1$, the SBCs of the real and imaginary parts always have an intersection point (Fig. 9), that is, the point defect cannot be directly eliminated. However, when k is large enough (about 0.92), the curvature of the SBC for the real part (at the defect point O_3) is large enough, so that the effect of the diffusion on this SBC will be strong enough. Eventually, under the effect of diffusion, point defect is removed from the medium along the SBC of the imaginary part.

5. Discussion and conclusion

In conclusion, we have presented a simple method to clear off spiral waves in three models of cardiac muscle by applying a global instantaneous disturbance. We have observed that the spiral wave can be eliminated in a short time, and then, the medium reaches the homogeneous oscillation in about one oscillation period. During this elimination, different from other methods, the oscillation frequency of the medium does not increase, but decreases directly and rapidly. In our method, we can eliminate the spiral wave by increasing the membrane potential globally. This increase is less than the amplitude of the membrane potential (about 80 mV). In addition, our method can eliminate the spiral wave within a short period of time. We believe that the method in this paper can provide a better guide to the clinical treatment of VT and VF.

The traditional method for treating the VT and VF events in the clinic is electroshock that stimulates the thoracic cavity with high voltage electricity (about 4–7 kV). This method brings great pain to the patient and cause great damage to heart tissue and other tissues of the human body.[18] It is widely believed that spirals in cardiac muscle are play a vital role in life-threatening situations (VT and VF).[4,5] Therefore, experts and scholars have conducted a lot of research on how to remove and suppress spiral waves. By most previous methods of the expulsion of spiral waves,[19,29–33] a target wave was created after applying a periodic forcing at a local point, which leads to the removal of the spiral wave from the heart. A target wave whose frequency is lower than that of the spiral wave cannot suppress the spiral wave, and a target wave with a higher frequency is required to suppress the spiral wave.[35,36] However, the emergence of the target wave with a higher frequency will cause the heartbeat to be accelerated again, which will aggravate the VT and directly endanger life. Accordingly, these methods are not clinically feasible. In this article, in the process of eliminating the spiral wave, the frequency of the medium is not increased again.

It is possible to effectively eliminate spiral waves and pinned spiral waves in cardiac tissue by applying a global pulse to increase the trans-membrane potential. Note that the value of the parameter k must exceed the threshold $\bar{k}_2 = 0.76$, otherwise more spiral waves will be generated (Fig. 2(a)), making the VT and VF events more serious.

About the control of spiral tip, Liu *et al.*[43] have studied the motion of spiral tip controlled by a local periodic forcing imposed on a region around the spiral tip in an excitable medium, and observed three types of trajectories of spiral tip. Chen *et al.*[44] moved the spiral tip by propagation time delay. In fact, using the method in this article can also make the spiral tip move. Therefore, the use of periodic pulses can make the spiral tip meander, and by adjusting the time interval between pulses, different trajectories of spiral tip can be obtained.

References

[1] Zipes D P, Heger J J and Prystowsky E N 1998 *Circulation* **98** 2334
[2] Xie Y, Grandi E and Bers D M 2014 *Europace* **16** 452
[3] Harada M, Honjo H and Yamazaki M 2008 *Am. J. Physiol.: Heart Circ. Physiol.* **294** H1896
[4] Winfree A T 1998 *Chaos* **8** 1
[5] Witkowski F X, Leon L J and Penkoske P A 1998 *Nature* **392** 78

[6] Lee J J, Kamjoo K and Hough D 1996 *Circ. Res.* **78** 660
[7] Garfinkel A, Kim Y H and Voroshilovsky O 2000 *Proc. Natl. Acad. Sci. USA* **97** 6061
[8] Cysyk J and Tung L 2008 *Biophys. J.* **94** 1533
[9] Shiferaw Y, Qu Z and Garfinkel A 2010 *Ann. NY Acad. Sci.* **1080** 376
[10] Karma A 1994 *Chaos* **4** 461
[11] Steinbock O, Schütze J and Muller S C 1992 *Phys. Rev. Lett.* **68** 248
[12] Hu G, Xiao J and Chua L O 1998 *Phys. Rev. Lett.* **80** 1884
[13] Xiao J, Hu G, Yang J and Gao J 1998 *Phys. Rev. Lett.* **81** 5314
[14] Sinha S, Pande A and Pandit R 2001 *Phys. Rev. Lett.* **86** 3678
[15] Kim M, Bertram M and Pollmann M 2001 *Science* **292** 1357
[16] Witkowski F X, Leon L J, Penkoske P A, Giles W R, Spano M L, Ditto W L and Winfree A T 1998 *Nature* **392** 78
[17] Weise L and Panfilov A 2017 *Phys. Rev. Lett.* **119** 108101
[18] Lown B 2001 *ACC Curr. J. Rev.* **10** 69
[19] Gao X and Zhang H 2014 *Phys. Rev. E* **89** 062928
[20] Wang C N, Ma J and Liu Y, Chaos control 2012 *Nonlinear Dyn.* **67** 139
[21] Ma J, Jia Y and Yi M 2009 *Chaos Soliton Fract.* **41** 1331
[22] Wu F, Wang C, Xu Y and Ma J 2016 *Sci. Rep.* **6** 28
[23] Ma J, Wu F and Hayat T 2017 *Physica A* **486** 508
[24] Zhang Q L, Ling L and Zhang Y 2011 *Chin. Phys. B* **20** 090514
[25] Pan D, Gao X and Feng X 2016 *Sci. Rep.* **6** 21876
[26] Chen J X, Guo M M and Ma J 2016 *Europhys. Lett.* **113** 38004
[27] Chen J X, Peng L and Ma J 2014 *Europhys. Lett.* **107** 38001
[28] Chen J X, Peng L and Zheng Q, Zhao Y H and Ying H P 2014 *Chaos* **24** 033103
[29] Aranson I, Levine H and Tsimring L 1994 *Phys. Rev. Lett.* **72** 2561
[30] Zhang H, Hu B, Hu G, Ouyang Q and Kurths J 2002 *Phys. Rev. E* **66** 046303
[31] Jiang M, Wang X and Ouyang Q 2004 *Phys. Rev. E* **69** 056202
[32] Lee J K 1997 *Phys. Rev. Lett.* **79** 2907
[33] Fu Y, Zhang H and Cao Z 2005 *Phys. Rev. E* **72** 046206
[34] Liu F C, Wang X F, Li X C and Dong L F 2007 *Chin. Phys.* **16** 2640
[35] Cui X, Huang X and Hu G 2015 *Sci. Rep.* **6** 34591
[36] Cui X, Huang X and Di Z 2015 *Europhys. Lett.* **112** 54003
[37] Cherry E M and Fenton F H 2008 *New J. Phys.* **10** 125016
[38] Gray R A, Wikswo P J and Otani F N 2009 *Chaos* **19** 033118
[39] Bär M and Eiswirth M 1993 *Phys. Rev. E* **48** R1635
[40] Aranson I and Kramer L 2001 *Rev. Mod. Phys.* **74** 99
[41] Zhang S, Bambi H and Zhang H 2003 *Phys. Rev. E* **67** 016214
[42] Cai M C, Pan J T and Zhang H 2014 *Phys. Rev. E* **89** 022920
[43] Liu G Q and Ying H P 2014 *Chin. Phys. B* **23** 050502
[44] Chen J X, Xiao J, Qiao L Y and Xu J R 2018 *Commun. Nonlinear Sci. Numer. Simulat.* **59** 331